Preliminary Quantitative and Qualitative Investigations on the Heterogeneous, Irreversible Uptake of Acetone by Titanium(IV) Oxide

John S. André
University of Michigan

Natalie Eskandary
Humbolt State University

Terry Franklin
Humboldt State University

Emilia J. McCann
Humboldt State University

Oscar Pascual-Diaz
Humboldt State University

Preliminary Quantitative and Qualitative Investigations on the Heterogeneous, Irreversible Uptake of Acetone by Titanium(IV) Oxide

Authors

John S. André, Natalie Eskandary, Terry Franklin, Emilia J. McCann, Oscar Pascual-Diaz, Gregory M. Pitch, Jesus D. Rincon, Megan N. Wright, and Christopher W. Harmon

Preliminary Quantitative and Qualitative Investigations on the Heterogeneous, Irreversible Uptake of Acetone by Titanium(IV) Oxide

John S. André (University of Michigan), Natalie Eskandary (Humbolt State University), Terry Franklin (Humboldt State University), Emilia J. McCann (Humboldt State University), Oscar Pascual-Diaz (Humboldt State University), Gregory M. Pitch (University of California, Santa Cruz), Jesus D. Rincon (Humboldt State University), Megan N. Wright (Humboldt State University), Christopher W. Harmon (Humboldt State University)

Keywords: atmospheric chemistry, heterogeneous, uptake, adsorption, desorption, DRIFTS, FTIR

Introduction

Heterogeneous chemical reactions are ubiquitous in the atmosphere and play a strong role in its chemical composition and physical properties.[1-2] Aerosols and/or solid environmental surfaces can alter the chemical composition of the atmosphere by promoting specific reaction pathways that are unique to the surface and their interaction with the gas phase.[3-4] Understanding how heterogeneous chemical reactions alter the physical and chemical properties of the atmosphere is critically important, as these reactions play many roles in the climate system. For example, heterogeneous reactions often increase the hygroscopicity (the capacity of a material to absorb water from the air) of organic aerosols and improve cloud nucleation.[5] The nucleation of clouds by atmospheric aerosols and their effect on light scattering (i.e., the indirect effect) represents one of the largest uncertainties in global climate models.[6-7] Additionally, the direct effect aerosols have on scattering Earth-bound solar radiation also represents a large uncertainty in climate models.[6-7] These reactions can also lead to organic and inorganic aerosols that have deleterious effects on human health.[8] Thus, continued research of heterogeneous reactions on atmospheric aerosols and environmental surfaces is critical as, despite the numerous studies already conducted, many uncertainties in large scale climate models still remain.[7]

The focus of this investigation is the reactive and irreversible uptake of volatile organic compounds (VOC) on environmental metal oxides

(EMO), the principle component of mineral dust. Many studies (see references 3, 4, 10 and references therein) to date have examined the reactivity of EMO and researchers have found them to be important in atmospheric chemistry. For example, long before the heterogeneous chemistry of anthropogenic origins plagued air quality, ice core samples demonstrated that aerosols from mineral dust circled the globe for hundreds of millennia.[9] Mineral dust is largely composed of inorganic compounds, and metal oxides are often the dominant species.[4] Unlike in the chemistry of organic aerosols, metal oxides such as titanium(IV) oxide, TiO_2, are well known for their photocatalytic (the acceleration of a reaction driven by light) and reactive properties. These properties are exploited in environmental remediation,[10] and it has been suggested that these properties could lead to unaccounted-for heterogeneous reactions in atmospheric climate models.[10-11] Indeed, TiO_2 has received much interest in the literature due to its unique catalytic and photocatalytic properties in heterogeneous atmospheric chemistry.[10] Still, despite the large number of studies, many unexplored research directions remain.[10] Conducting quantitative experiments under appropriate conditions of state and composition is the biggest challenge of these; this investigation describes pursuits toward that end.

The central hypothesis of this investigation is that small gas phase VOC can react on mineral dust aerosol surfaces and create larger compounds that are more likely to stick to the surface. These larger compounds would then be transported long distances to regions of the world where they may not be accounted for. The presence of such an organic surface layer will then alter chemical and physical properties of mineral dust aerosols. Indeed, field studies have shown atmospheric mineral dusts are (in addition to complex mixtures of minerals, clays, nitrates, sulfates, etc.[4]) often complex mixtures of various water soluble organic acids,[12] which can form organic salts[13] after being *aged*. We hypothesize the creation of such a layer is condition specific and seek to quantify the formation of such a layer under appropriate condi-

tions of state and composition. Most quantitative information on VOC reactive uptake is conducted under highly idealized conditions of temperature, pressure, and composition. Therefore, we seek to investigate the formation of organic layers on the surface of tailored mixtures of EMO and, eventually, actual dust samples. This investigation will assess the efficacy of mineral dust aerosol to take-up VOC and form an organic layer under actual atmospheric aging conditions of state and composition. Preliminary qualitative and quantitative work is presented here using a baseline condition with a representative VOC (acetone) and EMO surface compound (TiO_2).

Mineral dust is eroded soil particles that have been become aloft in the atmosphere. They are the second largest contributor to the global aerosol burden, after sea spray aerosols.[14] The chemical composition of mineral dust is very similar, if not identical, to that of the crustal rock from which the dust originated.[15] Many locations around the world report mineral dust to be fairly uniform in composition (% by weight) with respect to SiO_2 (~60%) and Al_2O_3 (~10-15%). The lower abundance oxides, such as CaO (~6%), Fe_2O_3 (~5%), MgO (~4%), and TiO_2 (~1%), are variable depending on location.[16,15] Most notably and pertinent to this study is TiO_2, which despite having the lowest abundance is generally the most reactive due to its photocatalytic properties[10] and has the largest uptake coefficient (the probability that a molecular gas-surface collision leads to uptake of the gas by the solid) in comparison to those EMOs listed above.[17]

Carbonyl compounds are of interest in this study as they are among the most prevalent and reactive VOC in the atmosphere, arising mostly from photo-oxidation of their parent hydrocarbon.[10] For example, a field study identified the three most common (of 23) carbonyl compounds found in the Los Angeles troposphere to be formaldehyde, acetaldehyde, and acetone, with total carbonyl four-hour mixing ratios of 22–29 parts per billion by volume (ppbv).[18] Shown in Figure 1 is an example of a reaction that can occur through the EMO or acid initiated catalysis of VOC: an

Aldol condensation reaction occurring with carbonyl compounds to form larger molecular weight compounds.[17, 19-21] If the starting carbonyl is acetone, first mesityl oxide (an enone) can form and further reaction can lead to isophorone.[17, 19-21] Additionally, isophorone is known to undergo photodimerization under actinic wavelengths (~300 nm)[22] in aqueous solutions (not shown in Figure 1), leading to even larger surface compounds. Thus, the creation of an organic layer on EMO surfaces under atmospheric conditions is very possible.

An interesting observation in this reaction scheme is the creation of larger compounds via the formation of new carbon-carbon double bonds. Olefins are quite reactive in the atmosphere and are subject to oxidation via ozone or the hydroxyl radical. This suggests the reaction/irreversible uptake of carbonyl compounds on EMO could alter the chemical properties of mineral dust because new carbon-carbon double bonds on the surface will be a sink for ozone. These reaction schemes are also fundamentally interesting, as the O:C (oxygen to carbon) ratio is *decreasing* in contrast to the fundamentally accepted view that O:C ratio should increase with chemical aging in the atmosphere.[5] This also suggests such an organic layer could alter the physical properties of mineral dust because water uptake could be hindered with a decrease in O:C.[5]

The primary results presented here deal with sparingly small surface coverage layers (Θ, defined as the number of monolayers) of acetone being adsorbed (i.e., stuck) or desorbed (i.e., unstuck) from a TiO_2 surface. These investigations will establish the initial stages of testing our central research hypothesis described above, where quantitative information on the adsorption and desorption rates are presented. Additionally, qualitative investigations on the reaction of acetone over TiO_2 to form mesityl oxide (Figure 1) will also be addressed, as well as future directions of research.

Methods

The Diffuse Reflectance Infrared Fourier Transform Spectroscopy (DRIFTS) technique will be the principle analytical instrument used in this research, which has been used extensively in atmospheric chemistry research.[2] In brief, a powdered solid is loaded into a reaction chamber (inside the sampling compartment of a Fourier Transform Infrared Spectrometer, FTIR), where the gas phase environment over the surface of the sample can be manipulated. The sample chamber is outfitted with infrared (IR) transparent windows (Zinc Selenide, ZnSe) and the analysis beam is scattered diffusely off the sample surface, focused by a set of mirrors, and then analyzed by a detector. This allows a reaction to be conducted *in-situ* and to monitor changes to the surface in real time. The IR beam will only analyze the surface of the sample, typically about 1−10 μm deep on non-absorbing samples.[23] Challenges associated with the DRIFTS technique are related to particle size and uniformity as well as to a very low signal that is scattered diffusely off the surface. This makes using the technique quantitatively difficult. However, as long as particle sizes are in the micron range and don't change size significantly throughout a reaction, the technique can be used quantitatively.[24] Thus, the technique is ideal because we wish to use particles in the micron size range, which are more relevant to mineral dust in the atmosphere. Additionally, highly reflective (weakly absorbing between 4,000-400 cm^{-1}) powders are ideal for DRIFTS,[24] which EMO particles most certainly are.

Shown in Figure 2 is the experiment station for studying the reactive/irreversible uptake of VOC with EMO via the DRIFTS technique. This entire apparatus (as well as the majority of data presented here) was built and tested by undergraduate research students under the supervision and guidance of the principle investigator (PI).[25] Pictured in the top left corner of Figure 2 is the experiment station located on the 3rd floor of the Science A building on the Humboldt State University campus, where the Chemistry Department is located. The station is organized in three main areas: the FTIR, the manifold, and the computer for data acquisition.

The manifold is built in an instrument rack and is capable of being relocated, if necessary. In the manifold, gas flow is controlled via an MKS

Instruments Type 247D 4 channel readout and the corresponding MKS mass flow controllers (MFC – M100 B) of differing ranges, shown in Figure 2. All gases are UHP (ultra-high purity, >99.999% Airgas®) and are delivered via ¼" PTFE tubing with various Swagelok® connections. Channel 1 (MFC 1) is predominantly used for O_2, channel 3 (MFC 3) is predominantly used for N_2, and channel 2 (MFC 2) can use He or N_2, and all are controlled by switch valves depending on the experiment. Ozone (O_3) can be generated, if desired, in the manifold as depicted in Figure 2. A stream of gas-phase VOC is created by diluting the flow of an organic liquid from a syringe pump (KD Scientific, KDS-100) with the flow of UHP N_2 from MFC 3 (Figure 2). A 25 µL Hamilton syringe (gas-tight) is used with a septum inserted into a Swagelok® union tee and can generate reliable flow rates of 0.1–10 µL/hr. When a VOC is mixed with 100 SCCM (standard cubic centimeters per minute) of N_2 from MFC 3 at a syringe pump flow rate of 0.1 µL/hr, a stable mixing ratio of a nominal organic (molar mass ~75 g/mol, density ~0.8 g/mL) of 4 parts per million by volume (ppmv) can be generated after traversing the 25-foot mixing coil (Figure 2).

The TiO_2 samples were prepared for analysis by DRIFTS using a similar version of the grinding method described by Finlayson-Pitts et al.,[26-27] which is known to create fairly uniform particle sizes between 1–5 µm. Preliminary imaging studies have been conducted as The College of Natural Resources and Science (CNRS) instrument core contains a Scanning Electron Microscope (SEM, Quanta 250) available to properly trained undergraduate students. Figure 3 shows one example, which demonstrates that, after grinding, the particles are polydisperse in size with some being greater than ~1 µm and most being in the sub-micrometer regime. After grinding, the TiO_2 is stored in a crucible in an oven at 115 ^{0}C and is only exposed to atmosphere for very brief periods of time during loading into the spectrometer. In the quantitative studies presented here, five nearly identical samples were created, using the methods described above, to investigate the reproducibility of our methodologies. These samples where loaded into shallow (~3 mm deep) cylindrical sample cups with a surface area exposed to the gas phase, ideal for analysis via DRIFTS, where the physical properties of these samples are shown in Table 1 below.

TABLE 1: Physical Properties of TiO_2 Samples

Sample	Mass (mg)	Exposed Geometric Surface Area (mm²)
1	103.6	46.6
2	133.7	47.8
3	128.1	51.5
4	99.7	45.4
5	129.1	46.6

Pictured in the top right corner of Figure 2 is the DRIFTS cell (Spectra Tech Inc., 6106640), which consists of a flow-through manifold, vacuum line, heater block, thermocouple, and manifold for liquid coolant. All preliminary experiments have been conducted without heating or cooling the sample, at ~28^{0}C. The sample holder is outfitted with ZnSe optics to minimize damage due to exposure of ozone or water vapor, which can degrade salt optics such as KBr. Thus, the DRIFTS cell can maintain a desired environment over the surface of the sample. In a typical experiment, a mixture of gases from the manifold is delivered to the DRIFTS cell at 100. standard cubic centimeters per minute (SCCM) to avoid pressurizing the cell (DRIFT cell volume = 5.3 cm³, 1/16" Swagelok® connections), which is confirmed by measuring the flow rate before and after the cell. A flow of UHP purge gas air (Parker-Hannifin Spectra 30) is also delivered to the FTIR (Thermo Nicolet Inc., Avatar 370) continuously whether experiments are being conducted or not.

Uptake studies are initiated by recording a background single beam spectrum of TiO_2 after purging the sample with 100. SCCM of UHP N_2 for ~1 hour. Subsequent spectra are then recorded by ratioing new single beam spectra to the initial single beam spectrum using the Kubelka–Munk (KM) algorithm (preferred qualitative methodology)[28] or the standard Absorbance (A) algorithm (preferred quantitative methodology)[2] after a

change is imposed on the surface (i.e., uptake of VOC). Using this methodology, the spectra reveal dynamic processes occurring at the gas/solid interface.[26-28] Negative features in the spectra indicate that a functional group has left the surface or has been modified, whereas positive features in the spectra show that a new functional group has been created on the surface or an existing functional group has been modified.[26-28] A representative series of spectra is shown in Figure 2, where different colors indicate evolving oxidation times in a different experiment not discussed in this article. In nearly all experiments, anywhere from 100–250 scans are acquired and averaged into one spectrum with a resolution of 4 cm^{-1} using an intermediate interferometer speed (0.47 cm/s) and the largest gain, which maximizes instrument sensitivity but may degrade the signal to noise ratio.

Results

Shown in Figure 4 is KM DRIFTS spectra of the adsorption of 5 ppmv of acetone (purified by distillation) in the gas phase (N_2 only) on TiO_2. Spectra were recorded as described above, where acetone adsorption spectra were ratioed to TiO_2 that was purged with dry UHP N_2 for one hour. Table 2 also summarizes the results of acetone adsorbed to TiO_2, which are consistent with previous studies.[19-21, 29] Not shown in Table 2 is the negative peak at 3670 cm^{-1}, shown in Figure 4(c), which corresponds to modification of surface bound H_2O and OH groups on TiO_2 as a result of

acetone adsorption. This peak is consistent with other observations[19-21, 29] and is a good indication that the spectra, shown in Figure 5, arise from irreversibly, adsorbed acetone.

Shown in Figure 5 is a representative quantitative experiment (Sample #5), where spectra were recorded in Absorbance mode. The experimental data shown in Figure 5 was acquired as described above, where a series of single beam spectra are ratioed at various time intervals as acetone is flowing over the surface of TiO_2. The manifold has a bypass 3-way valve (not pictured in Figure 2), where a stable mixing ratio of acetone can be established and exhausted to a fume hood prior to exposure to the sample surface in the DRIFTS cell. This allows us to initially establish a clean and dry single beam background spectrum and switch the bypass valve from *exhaust mode* to *exposure mode*, which establishes the beginning of a kinetic experiment (i.e., *time* = 0). Adsorption studies are initiated by switching from exhaust mode to exposure mode and are conducted for ~1 hour using approximately 50 ppmv of acetone, after which time desorption studies are initiated by switching the valve back to exhaust mode. Thus, each time an adsorption experiment was conducted a desorption experiment followed immediately, where the sample is purged with UHP N_2 only and ratioed to the same initial single beam background prior to any acetone exposure.

Each of the samples shown in Table 1 were tested twice, where an adsorption study was initiated, as described above, followed immediately by

TABLE 2: Peak Assignments of Acetone Adsorbed on TiO_2

Vibration Mode	Frequency (cm^{-1}) This Work	Frequency (cm^{-1}) Literature	References
ν(C–H)	2972	2971–2973	[19-21, 29]
ν(C=O)	1703, 1693	1688–1702	[19-21, 29]
ν(C–C)	1240	1238–1243	[19-21, 29]
δ_{as}(CH$_3$)	1423	1420–1422	[19-21, 29]
δ_s(CH$_3$)	1365	1365–1368	[19-21, 29]

a desorption study. Interestingly, all samples tested (and their respective trial replicates) showed very similar behavior to that seen in Figure 5 with the exception of sample #2, which did not demonstrate any level of acetone adsorption. While the behavior of each sample (less #2) was very similar, with respect to adsorption/desorption of acetone, the absolute absorbance data was not identical. For example, Figure 6(a) shows the first trial replicate peak absorbance for samples #1, 3, 4, & 5 in adsorption mode (note, sample #2 is not shown as no adsorption or desorption was detected). As shown in Figure 6(a), the *absolute* peak absorbance from sample to sample is not the same; however, when the data is *normalized* the adsorption and desorption data from sample to sample is very consistent, shown in Figure 6(b). This was done by normalizing the area under the curve between $1740–1660$ cm^{-1} (i.e., the carbonyl region) in spectra, recorded just prior to switching to exhaust/desorption mode. Error bars arise in this analysis from also averaging in the normalized peak absorbance. In this methodology, all experiments will achieve adsorption equilibrium at a normalized value of 1.0 and the desorption equilibrium value is unknown *a priori*. Predictive models for adsorption and desorption are also shown as solid lines and shaded areas in Figure 6(a,b), which will be discussed in more detail below.

When a large surface density of acetone molecules are present $(\Theta > 0.3)$[19-21, 29], they are in close enough proximity to each other to undergo an Aldol condensation, leading to the formation of mesityl oxide and possibly isophorone as shown in Figure 1. This result has been reasonably corroborated and is shown in Figure 7. In this experiment a large (qualitative, unknown *a priori*) amount of acetone was passed over the surface of TiO$_2$ in the DRIFTS cell for ~60 minutes, where similar behavior as that seen in Figure 5 was observed. However, when the experiment was switched into desorption mode (by purging the surface with UHP N$_2$) the spectra revealed a chemical change as seen in Figure 7(a,b).

The classic text-book[30] acid-catalyzed aldol condensation reaction mechanism is shown in Figure 7(c) to assess if the spectra shown in Figure

7(a,b) are evidence of mesityl oxide formation. In step 1 of the mechanism, acid catalyzed enolization occurs via protonation of the carbonyl group, leading to the production of water and an electrophilic protonated ketone (i.e., the conjugate acid of acetone). Some of those conjugate acids can undergo further proton transfer reactions with available water molecules to create a stable enol, which will act as a nucleophile (i.e., Lewis base) and attack the carbonyl carbon of the electrophilic protonated ketone shown by step 2. The first two steps in the mechanism are critical, as they are what create new carbon-carbon bonds, owing to the creation of larger molecular weight compounds. The evolution of function groups in DRIFTS spectra from $0–17$ minutes suggests this mechanism (or something similar) is occurring on the surface of the TiO$_2$ particles. As can be seen in Figure 7(a), from $0–7$ minutes the surface hydroxyl peak (3670 cm^{-1}) reduced in intensity while a new band most likely associated with water $(\nu_s/\nu_{as}, 3412$ cm$^{-1})$ appeared. This is evidenced with the protonation of the ketone group and production of water in step 1. Additionally, from $0–7$ minutes Figure 7(b) shows a drastic reduction in the intensity of the carbonyl peak $(\nu(C=O), 1703$ cm$^{-1})$ with the appearance of a shoulder at 1666 cm^{-1}. As the spectra evolve from $7–17$ minutes the carbonyl peak completely disappears, consistent with the nucleophilic attack of the enol on the conjugate acid leading to the creation of an α-hydroxy carbocation shown by step 3. Additionally, $\nu(C–H)$ and $\delta(CH_3)$ features $(3,000–2800$ and 1447 cm^{-1}, respectively) are seen during this time interval, which is also consistent with steps 2 and 3. As the spectra evolve from $17–57$ minutes it becomes difficult to discern the mechanism and associated functional groups. For example, previous researchers have assigned adsorbed mesityl oxide $\nu(C=C)$ and $\nu(C=O)$ to be 1602 and 1666 cm^{-1}, respectively[29], which we do see in our spectra; however, the intensity of both of these peaks should be very similar. Figure 6(d) shows a NIST reference spectra of mesityl oxide vapor,[31] where the intensities of both $\nu(C=C)$ and $\nu(C=O)$ are similar (albeit shifted ~30 cm^{-1} higher due to it being a gas). Indeed, previous researchers also see similar intensities in both $\nu(C=C)$ and

$\nu(C=O)$ for adsorbed mesityl oxide.[29] Thus, it is unclear if these spectra are in fact confirmation of mesityl oxide formation or if we are just limited by an older, less sensitive instrument. Similarly, the NIST reference spectra of isophorone vapor[31] is also shown, which is a potential product that could form through further acid catalyzed (or surface catalyzed) Aldol condensation reaction mechanisms.[17] The $\nu(C=O)$ peak at 1694 cm^{-1} (likely shifted to around ~1660 cm^{-1} in the adsorbed phase) should be much more prominent than the $\nu(C=C)$, which does not appear to be the case in the DRIFTS spectra shown in Figure 7(a,b) either. These observations raise the question if they are from a limitation of our instrument or actual differences in the observed chemistry. Further investigations are most certainly warranted.

Discussion

The combination of qualitative and quantitative data, shown above, represents a baseline level of progress towards investigating our central hypothesis: that small gas phase VOC can stick and react on mineral dust aerosol surfaces, which will create larger compounds that can modify the physical and chemical properties of such mineral dust. The efficacy at which these VOC adsorb (i.e., stick) and desorb, we predict, is highly dependent on the surface conditions present in a sample, such as its surface area, crystal structure, what is has been exposed to prior to VOC exposure, etc.

Thus, a number of quantitative parameters can be used to compare each of these condition specific adsorption/desorption profiles; however, 1st order rate constants for adsorption/desorption will be the principle quantitative parameter that is presented for now.

A simple 1st order kinetic model approaching equilibrium was fit to the data, shown by equation 1, where $[A]_t$, $[A]_e$ and $[A]_0$ can represent the normalized or un-normalized concentrations at any time (t), equilibrium, and initially ($t=0$), respectively, k is the first order rate constant, and t is time in minutes.

$$[A]_t = [A]_e + ([A]_0 - [A]_e)e^{-kt} \tag{1}$$

This model can be applied to the adsorption or desorption studies, where in the adsorption studies the theoretical normalized value for $[A]_e$ and $[A]_0$ are 1 and 0, respectively, thus making equation 1: $1-e^{-kt}$. In the desorption studies the theoretical values for $[A]_e$ are unknown *a priori* and that of $[A]_0$ should be 1. These predictive models are shown as solid lines in Figure 6(a) for each respective sample (where values are not normalized) as well as for the entire normalized data set in Figure 6(b). In each of these parameterizations the rate constants, k, should be very similar; however, the equilibrium and initial values ($[A]_e$ and $[A]_0$, respectively) will obviously be different whether the data has been normalized or not.

TABLE 3: Summary of fit parameters[a] given by equation 1

Sample	Adsorption k (min^{-1})	Adsorption $[A]_e$	Adsorption $[A]_0$	Desorption k (min^{-1})	Desorption $[A]_e$	Desorption $[A]_0$
1	0.124±0.023	0.958±0.029	0.013±0.090	0.0405±0.0230	0.741±0.036	0.965±0.216
3	0.117±0.018	0.968±0.035	0.006±0.073	–	–	–
4	0.133±0.043	1.042±0.060	0.026±0.152	0.0436±0.0161	0.669±0.042	0.983±0.146
5	0.112±0.018	1.006±0.033	-0.032±0.069	0.0503±0.0223	0.629±0.054	0.998±0.181
All	0.116±0.014	0.957±0.022	0.032±0.056	0.0631±0.0262	0.716±0.029	0.993±0.171

[a] Fit parameters are conducted at the 95% confidence interval

Summarized in Table 3 are results for the 1st trial replicate of the normalized results and their respective quantitative parameters (note, due to technical errors the desorption data for Sample 3 was not able to be analyzed; however, did proceed very similarly as the other data sets).

The results are presented as individual samples as well as for all data (i.e., "All"), which is the exact same data that is seen in Figure 6(b). As can be seen in Table 3, the theoretical values for $[A]_e$ and $[A]_0$ with respect to adsorption, are as exactly as they should be, barring some amount of data fitting error associated with the very low signal present in spectra. Additionally, all rate constants for both adsorption and desorption studies are self-consistent with each other and within the 95% confidence interval.

Most interesting for this study is the difference between adsorption and desorption rate constants, where, consistently, the adsorption rate constant is nearly double that of the desorption rate constant. Applying fundamental concepts of equilibrium to this observation, a simple equilibrium constant (K_{eq}) and corresponding change in Gibbs Free Energy (ΔG) can be calculated, which is shown by equation 2.[32] Here k_{ad} and k_{des} represent the adsorption (i.e., *forward*) and desorption (i.e. *reverse*) rate constants, respectively, R is the universal gas constants in units of J mol^{-1} K^{-1}, and T is the temperature in units of K.

$$\frac{k_{ad}}{k_{des}} = K_{eq} = e^{-\Delta G/RT} \qquad (2)$$

Using this equation K_{eq} is calculated to be (for ALL data) 1.84 ± 0.80 and ΔG (at 287 K, the average planet-wide temperature) is -1.51 ± 0.66 kJ mol^{-1}. Despite the fact that there is fairly large error in these parameters (~40%), the sign and magnitude are significant and confirm our central hypothesis that small VOC can stick to the surface of EMO. For example, a negative Gibbs Free energy (correspondingly, an equilibrium constant greater than 1) suggests acetone will spontaneously stick to an EMO surface at most atmospheric temperatures.[32] This is confirmed by the fact that the equilibrium

parameter value (i.e., $[A]_e$) in the desorption studies is 0.716 ± 0.029, which means, on average, after acetone has spontaneously stuck itself to a surface (i.e., adsorption) roughly 68.7–74.5% will remain on the surface at equilibrium. Indeed, to test this observation all samples were left in the DRIFTS sample chamber overnight, after the ~1 hour of desorption studies, and 24-hours later the acetone signal was very similar, if not identical, to the last spectra recorded! This indeed confirms acetone attains an equilibrium surface coverage and will NOT reversibly desorb.

Conclusions and Future Directions

In this study we have shown that acetone, a VOC largely present in the atmosphere, can spontaneously and irreversible stick to a TiO_2 surface, which is a small, yet representative component of mineral dust aerosol. This *sticking* appears to be quite strong and, over atmospheric time scales of hours and days, may remain stuck to the mineral dust surface and be transported long distances to another part of the world, where it is perhaps not accounted for. Additionally, when the surface coverage of acetone is large (and unknown *a priori* in our experiments) it self-reacts via the Aldol Condensation mechanism and forms a larger compound that could change the surface properties of its host mineral dust.

The preliminary work we have presented here is significant to the atmospheric chemistry and air pollution community as we have shown small gas phase molecules, which are expected to remain in the gas phase, can stick irreversibly to solid aerosol (specifically mineral dust) surfaces. Given that the direct and indirect effects aerosols have on scattering Earth-bound solar radiation represents a large uncertainty in climate models[6-7], continued research on aerosols and their interaction with the atmosphere is desired. For example, the reactions shown here can modify the chemical and physical properties of mineral dust, making their role in the climate system less known. Additionally, adsorbed surface organic compounds (i.e., acetone, mesityl oxide, etc.) can also lead to aerosols that have deleterious effects on human

health.[8] Thus, continued research in this direction is critical as, despite the numerous studies already conducted, many uncertainties in large scale climate models and the effect atmospheric aerosols have on human health still remain.[7]

In the future, we wish to systematically *age* our EMO samples prior to any VOC adsorption/desorption by exposing those EMO samples to light, relative humidity, an oxidizing environment, etc., and measure how the adsorption/desorption rate constants with respect to acetone (or any other VOC) change as a result. These future experiments aim to mimic actual chemical and physical aging as it may occur in the real environment/atmosphere. Additionally, we also seek to quantify how the formation of mesityl oxide changes as a result of this *atmospheric aging*. We already have some evidence that suggests these types of surface processing or aging can make a big difference in the uptake of VOC. For example, Sample #2 consistently did not display any type of irreversible uptake or surface chem-

istry despite the fact that it was created identically to the other samples and looks identical as well. A simple hypothesis for this observation is that the surface of Sample #2 was inadvertently exposed or contaminated to some laboratory or atmospheric species, thus rendering its surface chemistry inert. Further investigation is most certainly desired. Last, we seek to gain even more quantitative information by gaining the ability to quantify the absolute number of molecules present on the surface. This will allow us to investigate the kinetic competition between irreversible adsorption/desorption and formation of mesityl oxide, which will be critically important to validate our hypothesis that the presence of large surface compounds can change the physical and chemical properties of the host mineral dust material. Investigating how the physical and chemical properties of mineral dust are altered by the presence of such surface compounds, is also a future direction of research in our group.
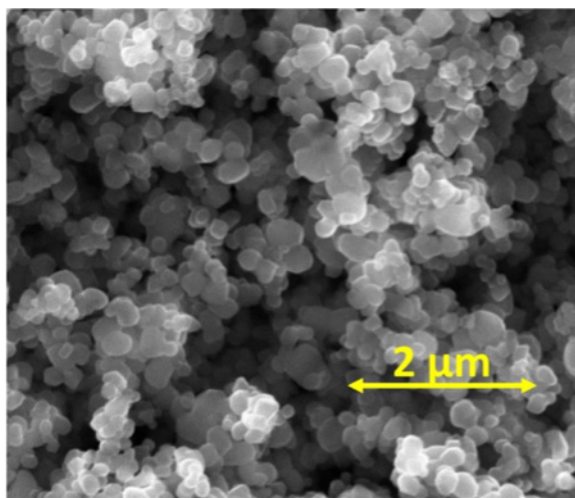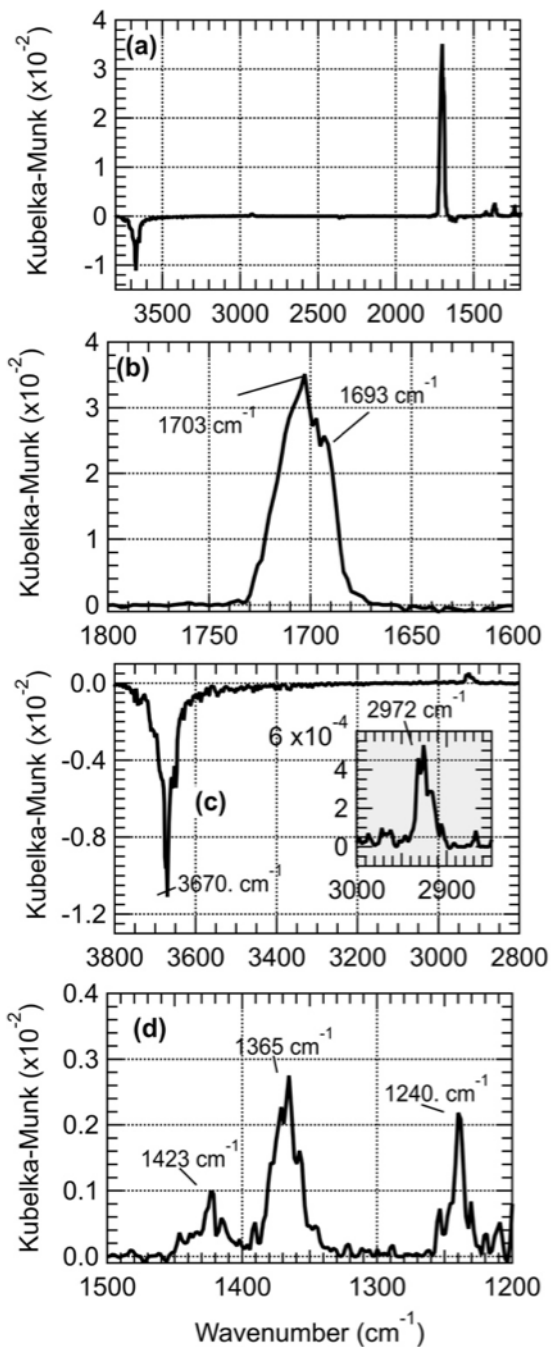
Figures
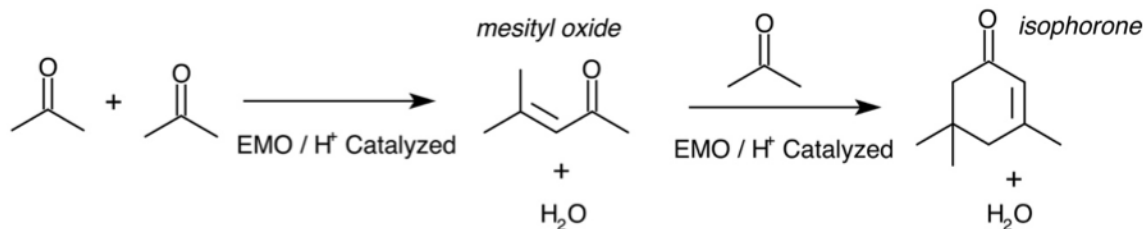
Figure 1: Acetone Aldol condensation occurring through EMO or acid catalyzed mechanisms.
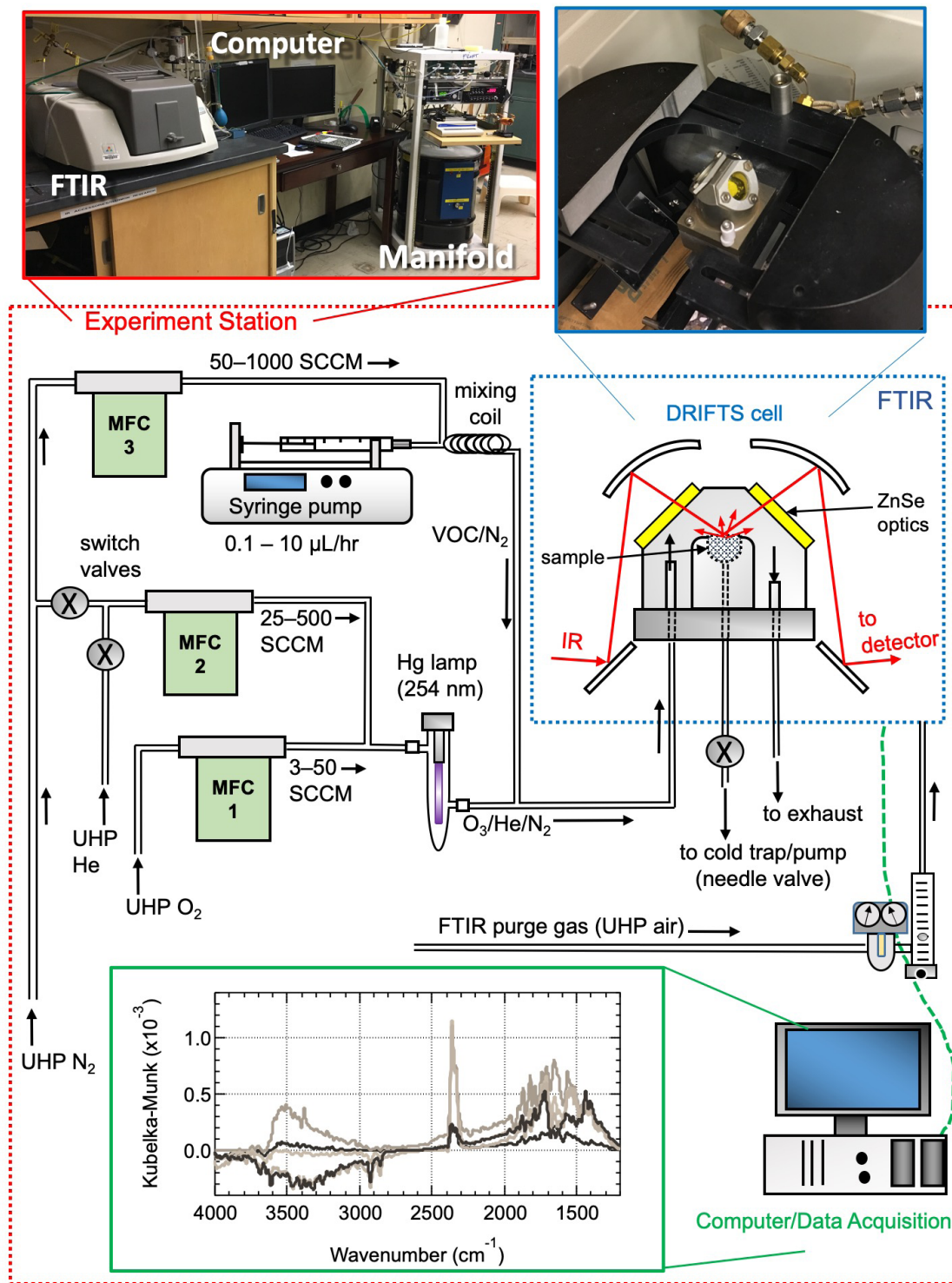
Figure 2: Experimental DRIFTS and manifold station. Key: VOC = volatile organic compound, MFC = mass flow controller, UHP = ultra-high purity, SCCM = standard cubic centimeter per minute, DRIFTS = diffuse reflectance infrared Fourier transform spectroscopy, IR = infrared.
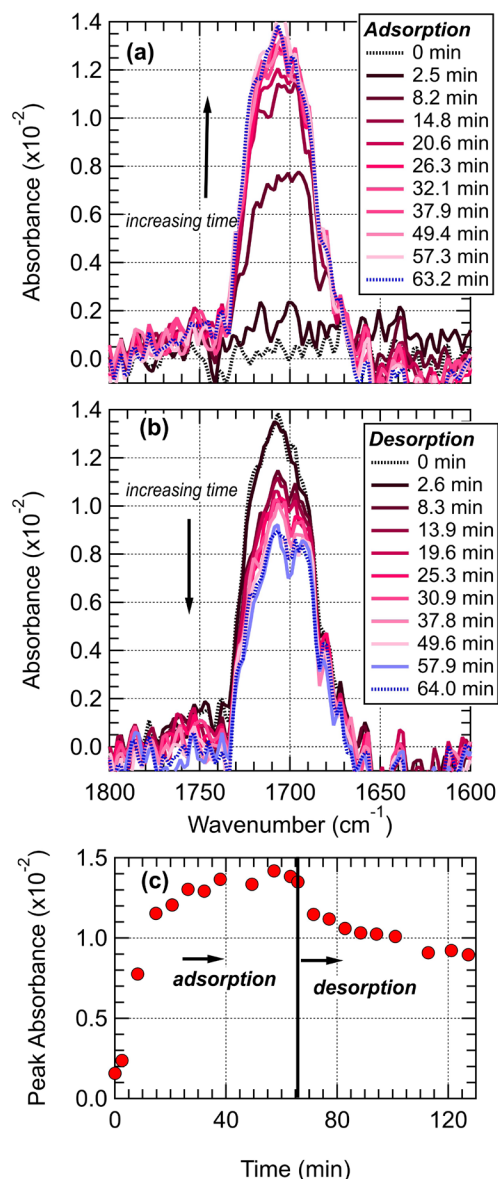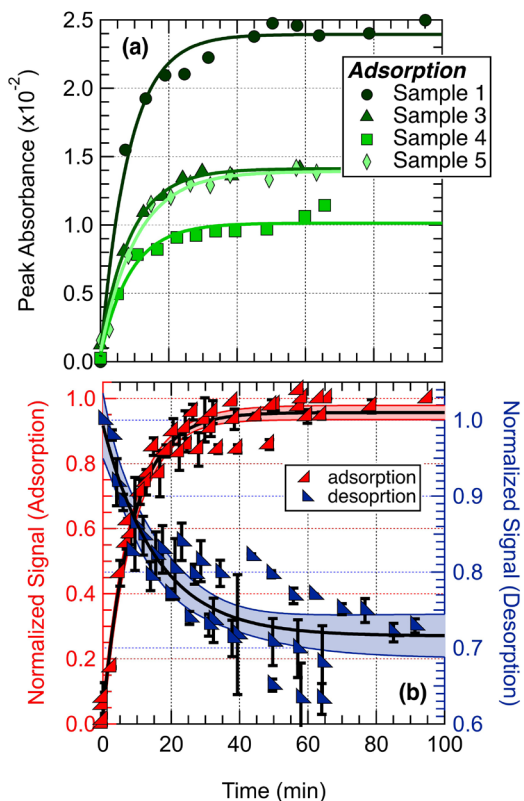
Figure 3: SEM Image of TiO_2 particles.

Figure 4(a): DRIFTS spectrum of ad-sorbed acetone (5 ppmv gas phase) on TiO_2. **(b)** carbonyl region, **(c)** O-H and C-H stretching region, **(d)** C-C and C-H region

Figure 6: **(a)** Peak absorbance of adsorbed acetone (50 ppmv gas phase) on TiO_2 as a function of time and sample. **(b)** Normalized absorbance signal (adsorption and desorption) as a function of time for Samples 1, 3, 4, & 5. In both **(a)** and **(b)** the data points are measured quantities whereas the solid lines (and shaded areas) are predictive models.
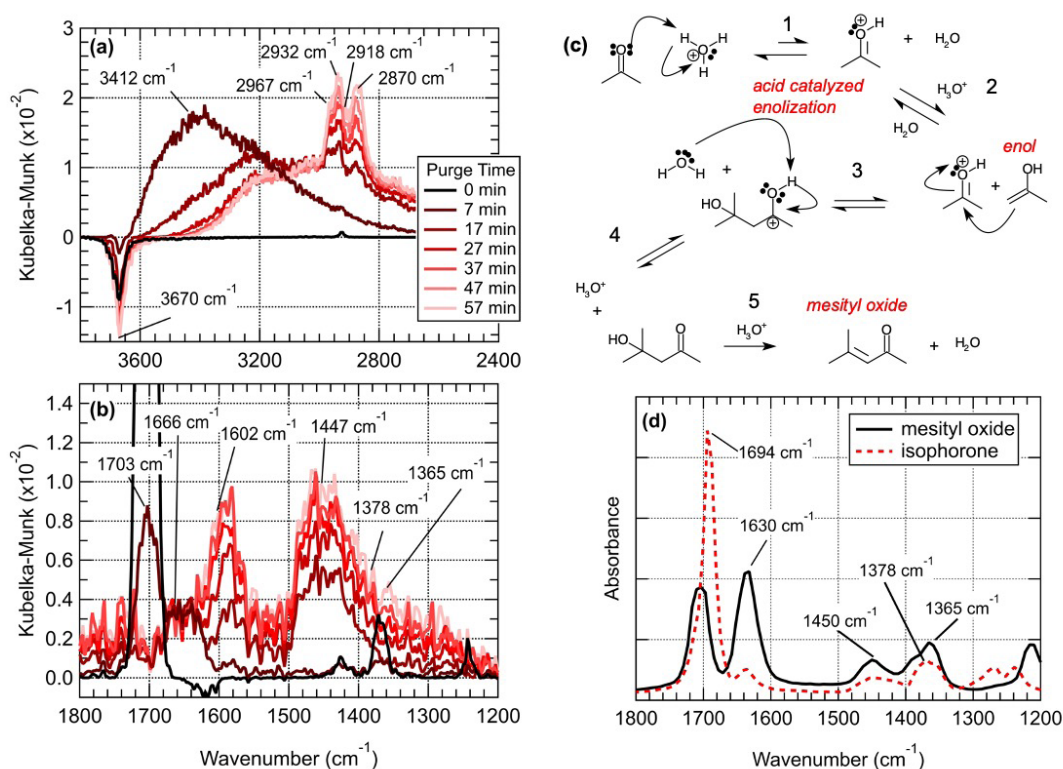
Figure 5(a): DRIFTS spectrum of adsorbed acetone (50 ppmv gas phase) on TiO_2 as a function of time. **(b)** Desorption of acetone (50 ppmv gas phase) on TiO_2 as a function of time. **(c)** Peak absorbance ($\sim$1700 cm^{-1}) as a function of total time (note, 63.2 min on adsorption graph = 0 min on desorption graph).

Figure 7(a,b): DRIFTS spectra of acetone reacting on a TiO$_2$ surface. **(c)** Text book acid-catalyzed Aldol condensation reaction. **(d)** NIST reference spectra of mesityl oxide and isophorone.

References

1. Finlayson-Pitts, B. J.; Pitts, J. N., *Chemistry of the Upper and Lower Atmosphere: Theory, Experiments, and Applications*. Academic Press: San Diego, 2000; p 1040 pp.

2. Finlayson-Pitts, B. J., Reactions at surfaces in the atmosphere: integration of experiments and theory as necessary (but not necessarily sufficient) for predicting the physical chemistry of aerosols. *Physical chemistry chemical physics : PCCP* **2009,** *11* (36), 7760-79.

3. George, C.; Ammann, M.; D'Anna, B.; Donaldson, D. J.; Nizkorodov, S. A., Heterogeneous photochemistry in the atmosphere. *Chem. Rev.* **2015,** *115* (10), 4218-58.

4. Usher, C. R.; Michel, A. E.; Grassian, V. H., Reactions on Mineral Dust. *Chem. Rev.* **2003,** *103* (12), 4883-4939.

5. Harmon, C. W.; Ruehl, C. R.; Cappa, C. D.; Wilson, K. R., A statistical description of the evolution of cloud condensation nuclei activity during the heterogeneous oxidation of squalane and bis(2-ethylhexyl) sebacate aerosol by hydroxyl radicals. *Physical chemistry chemical physics : PCCP* **2013,** *15* (24), 9679-93.

6. Myhre, G.; Shindell, D.; Bréon, F.-M.; Collins, W.; Fuglestvedt, J.; Huang, J.; Koch, D.; Lamarque, J. F.; Lee, D.; Mendoza, B.; Nakajima, T.; Robock, A.; Stephens, G.; Takemura, T.; Zhang, H., Anthropogenic and Natural Radiative Forcing. In *Climate Change 2013:*

The Physical Science Basis. Contribution of Working Group I to the Fifth Assessment Report of the Intergovermental Panel on Climate Change, Stocker, T. F.; Qin, D.; Plattner, G.-K.; Tignor, M.; Allen, S. K.; Boschung, J.; Nauels, A.; Xia, Y.; Bex, V.; Midgley, P. M., Eds. Cambring University Press: Cambrige, UK and New York, NY, USA, 2013.

7. IPCC, 2013: Summary for Policymakers. In *Climate Change 2013: The Physical Science Basis. Contribution of Working Group I to the Fifth Assessment Report of the Intergovermental Panel on Climate Change*, Stocker, T. F.; Qin, D.; Plattner, G.-K.; Tignor, M.; Allen, S. K.; Boschung, J.; Nauels, A.; Xia, T.; Bex, V.; Midgley, P. M., Eds. Cambridge University Press: Cambridge, UK and New York, NY, USA.

8. Samet, J. M.; Zeger, S. L.; Dominici, F.; Curriero, F.; Coursac, I.; Dockery, D. W.; Schwartz, J.; Zanobetti, A. *The National Morbidity, Mortality, and Air Pollution Study. Part II: Morbidity and mortality from air pollution in the United States*; Health Effects Institute: 2000; pp 5-70.

9. Kohfeld, K. E.; Harrison, S. P., DIRTMAP: the geological record of dust. *Earth-Sci. Rev.* **2001,** *54* (1–3), 81–114.

10. Chen, H.; Nanayakkara, C. E.; Grassian, V. H., Titanium dioxide photocatalysis in atmospheric chemistry. *Chem. Rev.* **2012,** *112* (11), 5919-48.

11. Parmon, V. N.; Zakharenko, V. S., Photocatalysis and Photosorption in the Earth's Atmosphere. *Catt* **2001,** *5* (2), 96–115.

12. Lee, S.-H.; Murphy, D. M.; Thomson, D. S.; Middlebrook, A. M., Chemical components of single particles measured with Particle Analysis by Laser Mass Spectrometry (PALMS) during hte Atlanta SuperSite Project: Focus on organic/sulfate, lead, soot, and mineral particles. *JGR* **2002,** *107* (D1).

13. Laskina, O.; Young, M. A.; Kleiber, P. D.; Grassian, V. H., Infrared spectroscopy and micro-Raman spectroscopy of select compoenents of mineral dust mixed with organic coating. *Journal of Geophysical Research Atomspheres* **2013,** *118*, 6593–6606.

14. Huneeus, N.; O., B.; Chevallier, F., Atmospheric Inverstion of SO2 and Primary Aerosol Emissions for the year 2010. *ACP* **2013,** *13*, 6555–6573.

15. Goudie, A. S.; Middleton, N., Saharan Dust Storms: Nature and Consequences. *Earth-Sci. Rev.* **2001,** *56*, 179–204.

16. Wedepohl, K. H., The composition of the continental crust. *Geochim. Cosmochim. Acta* **1995,** *59* (7), 1217–1232.

17. Li, P.; Perreau, K. A.; Covington, E.; Song, C. H.; Carmichael, G. R.; Grassian, V. H., Heterogeneous reactions of volatile organic compounds on oxide particles of the most abundant crustal elements: Surface reactions of acetaldehyde, acetone, and propionaldehyde on SiO2, Al2O3, Fe2O3, TiO2, and CaO. *JGR* **2001,** *106* (D6), 5517-5529.

18. Grosjean, E.; Grosjean, D.; Fraser, M. P.; Cass, G. R., Air Quality Model Evaluation Data for Organics. 2. C1–C14 Carbonlys in Los Angeles Air. *Environ. Sci. Technol.* **1996,** *30* (9), 2687–2703.

19. Maazawi, M. E.; Finken, A. N.; Nair, A. B.; Grassian, V. H., Adsorption and Photocatalyic Oxidation of Acetone on TiO2: An *in Situ* Transmission FTIR Study. *J. Catal.* **2000,** *191*, 138–146.

20. Griffiths, D. M.; Rochester, C., *Journal of the Chemical Society, Faraday Transactions 1: Physical Chemistry in Condensed Phases* **1978,** (74), 403.

21. Baraka, C.; Gravejat, P.; Guaitella, O.; Thevenet, F.; Rousseau, A., Oxidation of isopropanol and acetone adsorbed on TiO2 under plasma generated ozone flow: Gas phase and adsorbed species monitoring. *Appl. Catal., B* **2014,** *147* (302–313).

22. Gonçalves, H.; Robinet, G.; Barthelat, M.; Lattes, A., Supramolecularity and Photodimerization of Isophorone: FTIR and Moleclar Mechanics Studies. *The journal of physical chemistry. A* **1998,** *102*, 1279-1287.

23. Carmona-Quiroga, P. M.; Blanco-Varela, M. T.; Domingo, C.; Martinez-Ramirez, S., Effect of concentration, particle size and the presence of protective coatingsin DRIFT spectra of building materials. *Vib. Spectrosc* **2009,** *50*, 312-318.

24. Meunier, F. C., The power of quantitative kinetic studies of adsorbate reactivity by operando FTIR spectroscopy carried out at chemical potential steady-state. *Catal. Today* **2010,** *155*, 164-171.

25. Pitch, G. M.; Andre, J. S.; Davie, A. J.; Harmon, C. W., Investigations of Water Uptake on Sodium Acetate Trihydrate and Nonhydrate as Model Aerosol Surfaces Using the DRIFTS and ATR Techniques. *Proceedings of the National Conference for Undergraduate Research (NCUR)* **2015**, 300–310.

26. Vogt, R.; Finlayson-Pitts, B., Diffuse Reflectance Infrared Fourier Transform Spectroscopic (DRIFTS) Study of the Surface Reaction of NaCl with Gaseous NO2 and HNO3. *J. Phys. Chem.* **1994,** *98*, 3747–3755.

27. Dilbeck, C. W.; Finlayson-Pitts, B. J., Hydroxyl radical oxidation of phospholipid-coated NaCl particles. *Physical chemistry chemical physics : PCCP* **2013,** *15* (24), 9833-44.

28. Smith, B. C., *Fundamentals of Fourier Transform Infrared Spectroscopy, 2nd Edition*. 2 ed.; CRC Press: 2011.

29. Coronado, J. M.; Katoaka, S.; Isabel, T.; Anderson, M. A., Dynamic phenomena during the photocatalytic oxidation of ethanol and acetone over nanocrystalline TiO2: simultaneous FTIR analysis of gas and surface species. *J. Catal.* **2003,** *219*, 219–230.

30. Loudon, G. M., *Organic Chemsitry* 3rd ed.; The Benjamin/Cummings Publishing Company, Inc.: Redwood City, CA, 1995.

31. Smith, A. L., *The Coblentz Society Desk Book of Infrared Spectra*. 2 ed.; Kirkwood, MO, 1982.

32. Raff, L. M., *Principles of Physical Chemistry*. Prentice Hall: Upper Saddle River, NJ, 2001.